Carbohydrate Polymers 111 (2014) 80–88

Contents lists available at ScienceDirect

Carbohydrate Polymers

journal homepage: www.elsevier.com/locate/carbpol

The shear dependence of the methylcellulose gelation phenomena in aqueous solution and in ceramic paste

Matthias Knarr*, Roland Bayer

Dow Wolff Cellulosics GmbH, August Wolff Str. 13, D-29699 Bomlitz, Germany

ARTICLE INFO

Article history:
Received 21 February 2014
Received in revised form 17 April 2014
Accepted 20 April 2014
Available online 28 April 2014

Dedicated to Dr. Walter Bayer on the occasion of his 90th birthday on January 4, 2014.

Keywords:
Thermal gelation
Methylcellulose
Ceramic extrusion
Gelation temperature

ABSTRACT

The gelation temperature of methylcellulose (MC) in aqueous solutions as well as in aqueous ceramic paste depends on the applied shear. Rheological investigations in oscillation vs. shear mode show lower gelation temperature at low shear rates as for the corresponding angular frequencies. Above a critical shear rate the gelation temperature is shifted to higher temperatures. The paste extrusion process uses MC as a plasticizer and runs under high shear conditions. When extruding close to the gelation temperature of the MC in the paste, crack formation and other defects can occur. The upwards shift of the gelation temperature with increasing applied shear gives a larger temperature window during the extrusion process. The understanding of the shear influence on the gelation temperature is important to design the optimal process conditions.

1. Introduction

Cellulose ethers (CE), like methylcellulose (MC), are derived from cellulose, the most widespread polysaccharide in nature. Cellulose forms the primary structural component of plants and is made of repeat units of the anhydroglucose monomer. The cellulose molecule is a regular, rigid and straight chain without any branching. Each anhydroglucose unit contains three functional groups – the hydroxyl groups on carbon atoms 2, 3 and 6. These hydroxyl groups form a highly ordered network of hydrogen bonds. Cellulose itself is insoluble in water and in most organic solvents.

The insolubility in water is often referred to strong intermolecular hydrogen bonding between cellulose molecules. Medronho, Romano, Miguel, Stigsson, and Lindman (2012) revisited some fundamental polymer physicochemical aspects of the polymer and postulated, cellulose is significantly amphiphilic and hydrophobic interactions play also an important role with regard to the solubility. These findings are currently under debate especially while considering previous publications (Glasser et al., 2012).

Methylcellulose is one of the most important commercial cellulose ethers that has been used in food (Floury, Desrumaux, Axelos, & Legrand, 2003; Kandasamy, Varadharaju, Kalemullah, & Maladhi, 2012; Knarr, Adden, Anderson, & Hübner-Keese, 2012), pharmaceutical (Ford & Mitchell, 1995; Ford, 1999; Rogers & Wallick, 2012) as well as non-regulated applications like ceramic extrusion (Schuetz, 1986), fuel cells (Church, Sanders, Speyer, & Cochran, 2007; Pusz, Smirnova, Mohammadi, & Sammes, 2007), nano particle synthesis (Bhui & Misra, 2012; Bhui, Pyne, Sarkar, Bar, Sahoo, & Misra, 2011) and construction applications (Akthar & Evans, 2010; Ou, Ma, & Jian, 2012). One of the most important features is the thermo-reversible gelation performance strongly influenced by the degree of substitution (Bayer & Knarr, 2012).

From all classes of cellulose ether that contain methyl groups MC has the lowest gelation temperature. This can be a hindrance in some applications e.g. reduced water retention in dry mortars when applied at higher temperatures or extruded ceramic pastes with a high concentration of methylcellulose in the paste (Bayer & Lang, 2012a), however it can be an advantage in some like food applications (hindrance of boil-out of fruit fillings in baked and hot-served pastry).

The synthesis of MC was already described by Lilienfeld (1912a,b,c) and independently by Dreyfus (1912), the cold water solubility, the coagulation and precipitation by heating, was also

* Corresponding author. Tel.: +49 05161 44 2555.
E-mail address: mknarr@dow.com (M. Knarr).

http://dx.doi.org/10.1016/j.carbpol.2014.04.078
0144-8617/

described by Lilienfeld. In 1913, Denham and Woodhouse (1913) published a similar process to achieve methylcellulose derivatives. First systematic studies of the "inverse" sol–gel transformation of MC with increasing temperatures were conducted by Heymann (1935). The turbidity during the phase transition at that time was explained by a dehydration of the methylcellulose chains at high temperatures. Since then the thermo-reversible phase transition of MC in aqueous solutions has been extensively investigated by various techniques like Sarkar (1979) with rheological investigations, Desbrieres, Hirrien, and Rinaudo (1998) with calorimetric experiments on heterogeneous (commercial) vs. homogenous lab synthesized MC, Takahashi, Shimazaki, and Yamamoto (2001) via micro-differential scanning calorimetry & small-angle X-ray scattering. Wang and Li (2005) studied the impact of MC with different molar mass with DSC and rheology as well as the influence of a magnetic field, which showed slightly lower gelation temperatures (Wang, Li, Chen, & Yang, 2007). Funami et al. (2007) investigated the thermal aggregation of methylcellulose by static light scattering technique to trace the transition of its molecular size and shape upon heating, Nishida and Takahashi (2008) with polarized optical microscope (POM) and wide angle X-ray scattering (WAXS) and Takeshita, Saito, Miya, Takenaka, and Shiomi (2010) with small-angle X-ray scattering (SAXS) and light scattering (LS) techniques and applied speckle analysis on the LS profiles and found the observed gelation and phase separation are strongly coupled to each other.

Haque and Morris (1993) investigated the presence of crystalline structures in solutions at low temperatures which dissociated during heating and allowed the development of a different structure at higher temperatures.

According to Sarkar (1995), water at relatively low temperatures forms an ice-like structure around the hydrophobic groups, such as the methyl substituents. When the solution is heated, the water structure breaks down with an increase of entropy, thus allowing the hydrophobic groups to interact and cause gelation.

Kobayashi, Huang, and Lodge (1999) found out evidence of the weak supermolecular association or clustering at 20 °C of semi dilute methylcellulose solutions. This clustering was significantly enhanced as the temperature increased based on hydrophobic association. At higher temperatures, strong local segregation of polymer-rich and polymer-poor regions occurred.

Hirrien, Chevillard, Desbrières, Axelos, and Rinaudo (1998) and Desbrières, Hirrien, and Ross-Murphy (2000) described heterogeneities in solutions which become more and more important with superimposed temperatures. It has been further suggested that the gelation is mainly driven by hydrophobic interactions between highly substituted zones and the presence of trisubstituted units that are essential for gelation.

By X-ray diffraction patterns of MC gels Kato, Yokoyama, and Takahashi (1978) proved the network junction points of gels are crystalline and consist of trimethyl glucose units.

Li et al. (2001, 2002), Li (2002) reported the concept of hydrophobic effective units based on the dispersity in the degree of substitution along the cellulose chain. Therefore, the thermodynamic mechanism involved in the hydrophobic association during the gelation, has been explained as an entropy-driven process, that is mainly controlled by the thermally induced destruction of hydrogen bonds formed between water molecules and methylcellulose chains.

Previous studies have proved the effect of decreasing gelation temperatures with increasing MC concentrations (Kobayashi et al., 1999; Sarkar, 1979). Additionally, co-ingredients like salts according to the Hofmeister series (Hofmeister, 1888) or sugar and sugar alcohols in aqueous solutions decrease the gelation temperature, whereas alcohols as co-ingredients in aqueous solutions lead to higher gelation temperatures (Bain et al., 2012; Heymann, 1935; Iso and Yamamoto, 1970; Kundu & Kundu, 2001; Levy & Schwarz, 1958; Xu, Li, Zheng, Lam, & Hu, 2004).

One of the drawbacks of the previous investigations has been the absence of an applied shear during the gelation process which is often present in industrial application processes. Therefore, it has been the aim of this study to investigate whether there is an influence of an applied shear on the gelation properties of the MC, on the one hand dissolved in an aqueous solution and on the other hand in a ceramic paste extrusion formulation.

Aqueous ceramic paste extrusion with cellulose ethers like MC, is the main method to produce ceramic profiles for automotive and industrial applications like filters, catalysts, insulation tubes and others. It is well known that the gelation temperature of the methylcellulose in the paste is dependent on the same parameters as in solution (Schuetz, 1986; Bayer & Knarr, 2012). To date however, prediction of the paste gelation temperature without the effect of an applied shear remains imprecise.

2. Experimental part

Aqueous MC solutions were prepared by adding the MC (Methocel™ A4M, Dow Chemical Company) to water, stirring the solutions with an overhead lab stirrer at 1000 rpm for one hour while cooling the solutions with an ice/water mixture. These solutions were stored in a refrigerator at 5 °C overnight.

Rheological investigations were performed with an Anton Paar Physica MCR 501 rheometer, with a cup and bob geometry (CC-27). Oscillatory measurements were made at 20 °C for $\omega = 100–0.1\ \mathrm{rad\,s^{-1}}$ with 5 data points each decade. The strain (deformation) γ was been held constant at 2%, which is within the linear visco-elastic region.

Steady shear flow experiments were performed at 20 °C for $\dot{\gamma} = 0.1 - 1000\ \ \mathrm{s^{-1}}$ with 5 data points each decade. Only the MC solution at a concentration of 3% was investigated with a cone and plate geometry (CP50-1°).

Temperature sweep investigations were performed with a heating rate of $1\ ^\circ\mathrm{C\,min^{-1}}$ at the given angular frequencies of 0.1, 1, 10 & 100 $\mathrm{rad\,s^{-1}}$ and shear rates of 0.1, 1, 10 & 100 $\mathrm{s^{-1}}$ with 4 data points each minute.

Pastes were prepared in a 30 ml kneading cell W30 of a Brabender Plasti-Corder PL 2000 torque rheometer with metallic cover head and were cooled down to 4 °C. A homogeneous mixture of 40 g of cordierite precursor material (Imerys cordierite CP820M) and MC (Methocel™ A4M, Dow Chemical) was introduced into the cell and mixed with water dosed in portions with a syringe. Further homogenization was done at 20 rpm until a constant torque was reached. After a break of 5 min, the temperature ramp was started at a defined shear rate (counter rotating kneading blades rotation speed) and a heating rate of $3\ ^\circ\mathrm{C\,min^{-1}}$ (programmed at the thermostat).

For the extrusion trials the paste preparation was started by mixing the cordierite precursor material and MC in the dry state, spraying in water, and kneading at room temperature. For details see Bayer and Knarr (2012). After kneading, extrusion through a water-cooled single-screw extruder with inner screw diameter of 80 mm took place using a honeycomb profile with a cell density of 47 cells $\mathrm{cm^{-2}}$ (300 cells per square inch) following the temperature sweep method described in Bayer and Knarr (2012). During all trials, the feeder screw speed was kept slightly lower than the auger screw speed. The temperature sweep measurement was started by heating up the water in the extruder jacket with a thermostat, programmed to an upper limit of 97 °C (heating rate $3\ ^\circ\mathrm{C\,min^{-1}}$). The material was extruded through the die, discharged onto a conveyor belt and recycled into the feeder screw until the temperature reached 90 °C or the extruded cordierite paste lost its plasticity,

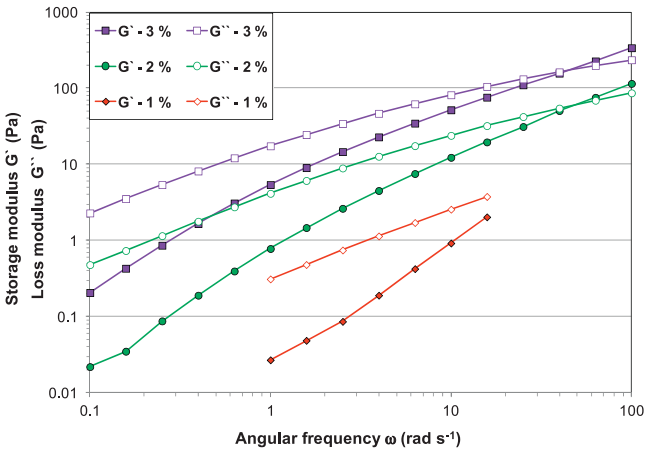

Fig. 1. Angular frequency ω dependence of the storage modulus G' and loss modulus G'' of MC at concentrations of 1%, 2% and 3% in aqueous solutions at 20 °C.

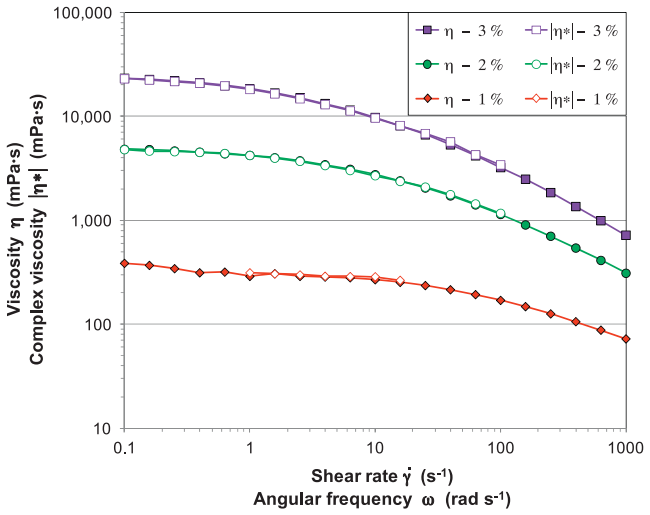

Fig. 2. Shear viscosity η and complex viscosity $|\eta^*|$ as a function of the shear rate $\dot{\gamma}$ and angular frequency ω of MC at concentrations of 1%, 2% and 3% in aqueous solutions at 20 °C.

got brittle or gave significant defects. The extrusion pressure was measured close to the die.

3. Results and discussion

3.1. Gelation behavior in aqueous solution

MC as well as most polysaccharide polymers is known to have strong viscosity enhancing (Staudinger & Schweitzer, 1930), as well as visco-elastic properties in solutions (Castelain, Doublier, & Lefebvre, 1987; Robinson, Ross-Murphy, & Morris, 1982). Prior to the analysis of the influence of different applied frequencies and shear rates on the gelation temperature, the impact of these parameters were investigated at a constant temperature. Fig. 1 shows the frequency dependence of the storage modulus, G', and the loss modulus, G'' (which characterize, respectively, elastic and viscous response) as a function of the concentration of a methylcellulose in aqueous solutions at 20 °C. All these experiments were conducted inside the linear visco-elastic region of the applied deformation.

Below the gelation temperatures of the MC solutions G' and G'' show strong dependencies of the angular frequency ω. At low frequencies, the loss modulus G'' is higher than the storage modulus G'. Deformation takes place so slowly that the majority of the energy is dissipated by viscous flow. The MC chains have time to respond to the externally imposed deformation by relaxing to an energetically more favorable state. As the frequency increases, the available relaxation time declines. The polymer chains can no longer slip past one another, so entanglements act more and more like fixed junctions. Consequently, the ability of this temporary polymer network to store the temporarily imposed energy increases, and it behaves more like an elastic solid. The storage modulus therefore increases more sharply with frequency than the loss modulus does (Clasen & Kulicke, 2001).

Due to a low network structure density at a concentration of $c = 1\%$ there is no cross-over of G' and G'' in the frequency domain for which reliable measurement data could be obtained. With increased concentration and polymer density the relaxation of the macromolecules gets hindered. This also leads to enhanced number of entanglements, increased absolute position of the moduli with increasing concentrations and a cross-over of the moduli can be detected in the high frequency region.

To further analyze the solution state of the polymers in solution, the data of the complex viscosity $|\eta^*|$ of the oscillation experiment were compared to the steady shear flow viscosity η. This follows the principles of the empirical Cox–Merz rule where equal values of $|\eta^*|$ and η for equivalent values of angular frequencies and shear rates were shown for melts or homogenous solutions (Cox & Merz, 1958). If a super architecture structure is present in the sample, η is lower than $|\eta^*|$ due to partial destruction of this structure with increasing applied shear (Kulicke & Porter, 1980).

Fig. 2 shows the plot of the complex viscosity $|\eta^*|$ as a function of the angular frequency and the shear viscosity η as a function of the shear rate $\dot{\gamma}$ for various MC concentrations in aqueous solutions at 20 °C, All solutions behave as non-Newtonian fluids. The polymer chains in solution form an entanglement network and at low shear rate, those entanglements which are disrupted by the imposed deformation are replaced by new interactions between different partners, with no net change in the extent of entanglements, and hence no reduction in viscosity. This situation corresponds to the horizontal Newtonian plateau in the low shear rate region. The onset of shear thinning occurs when the rate of externally imposed movement becomes greater than the rate of formation of new entanglements, and thus the crosslink density of the network is depleted and the viscosity decreases (Morris, Cutler, Ross-Murphy, Rees, & Price, 1981).

With increased concentration the viscosities grow and the shear thinning properties are enhanced. Due to the higher cellulose ether concentration, more and more entanglements are built-up between the polymer coils in solution. Evidence of the absence of super architecture structure in these aqueous MC solutions is given by the comparison of the complex viscosity $|\eta^*|$ vs. the shear viscosity η in Fig. 2. At this temperature of 20 °C far below the gelation temperature the Cox–Merz rule is fulfilled.

Methylcellulose solutions are known to form strong gels with increasing temperatures mainly driven by hydrophobic interactions (Fairclough et al., 2012; Liu, Joshi, Lam, & Tam, 2008). The gelation performance of various concentrations of MC in aqueous solutions is shown in Fig. 3 in terms of the storage modulus G' and the loss modulus G'' as functions of the temperature. The measurement conditions were chosen in the linear visco-elastic region to achieve a good signal to noise ratio, but also to avoid any destruction of the aggregates or associates during the gelation process.

The temperature dependence of the storage modulus G' and loss modulus G'' can be segmented into three zones. At low temperatures, the viscous parts are dominant in comparison to the elastic parts as also shown in Fig. 1. This represents the typical attributes of a viscous fluid with entanglements between the polymer chains in solution (Ross-Murphy, 1995). With increasing temperatures, the Brownian motion of the polymers increases

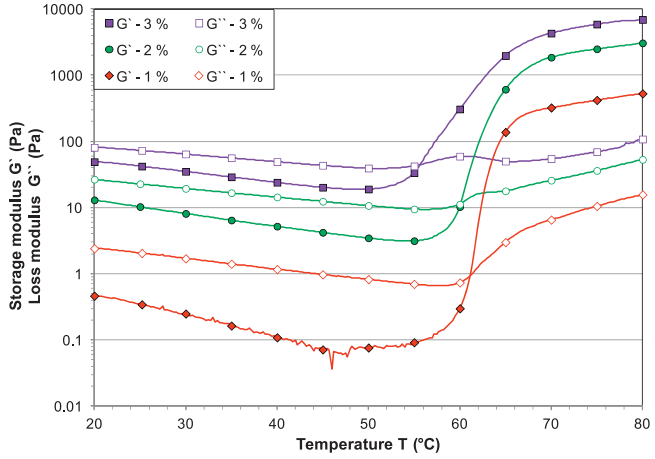

Fig. 3. Storage modulus G' and loss modulus G'' as a function of the temperature T of MC at concentrations of 1%, 2% and 3% in aqueous solutions (angular frequency $\omega = 10\,\mathrm{rad\,s^{-1}}$ and heating rate = 1 °C min^{-1}).

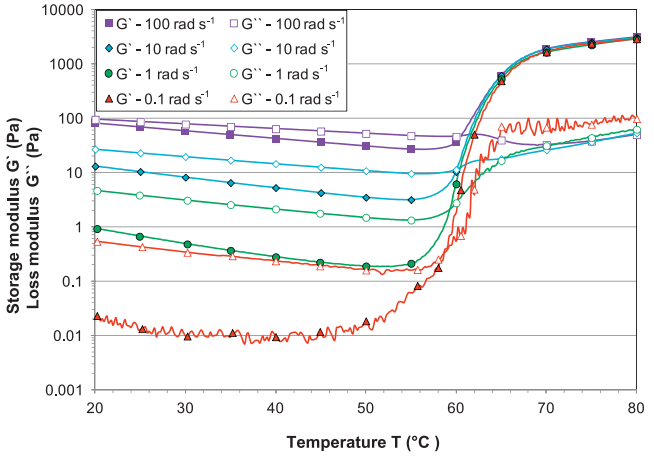

Fig. 4. Storage modulus G' and loss modulus G'' as a function of the temperature T of MC at concentrations of 2% for various angular frequencies ω in aqueous solutions (heating rate = 1 °C min^{-1}).

and the thermodynamic solvent quality decreases. Therefore, the moduli decrease and the storage modulus declines more as the loss modulus. Due to the increasing Brownian motion more entanglements between the polymer coils are released than reformed and so the temporary energy storage capacity is reduced. Additionally Haque and Morris (1993) described also an initial decrease in rigidity in the early stages of heating due to a loss of ordered structure. Therefore the observed reduction in the moduli could be caused by a combination of both effects.

At a specific temperature for each concentration the storage modulus G' shows a strong increase and the G' values become dominant over the loss modulus G''. At these temperatures the methylcellulose starts to build up a gel network. With increasing temperatures, the network structure is further increased. This is represented by the increase of the storage modulus values whereas the loss modulus only shows minor changes.

In the high temperature region, only a slight increase of the storage modulus is detected. The formation of the network structure is mostly completed and only minor changes take place.

Increasing concentrations generally show a shift of the gelation temperature to lower temperatures and a shift of the storage modulus as a representative of the gel strength in the high temperature region to higher values. The data were analyzed according to the minimum storage modulus G'_{min}, cross-over of $G' = G''$ and the highest slope during the gelation process. For this analysis the storage modulus was logarithmize and the minimum of the storage modulus G'_{min} was normalized to zero. The data were plotted on linear scale as a function of the temperature. For an increase of the storage modulus a subset of these G'_{norm} vs. temperature data (covering a range of 5 data points) was build up to achieve the largest magnitude slope from the complete curve. The midpoint of this temperature range was reported as the inflection, the slope of the linear fit as the slope at inflection, and the linear slope was used to extrapolate back to the baseline ($G'_{\mathrm{min}} = 0$) to get the onset gelation temperature. Additionally, the regression coefficient R^2 of this fit is given. All of these data for the concentration dependence of the gelation process are listed in Table 1 and underline the effect of decreasing gelation temperatures with increasing concentration. The concentration effect was in good agreement with previous published results (Sarkar, 1979; Kobayashi et al., 1999). Additionally, a decreasing slope of the gelation curves with increasing concentration was observed. The polymer density in solution increased with concentration and therefore the availability of junction points for the gelation process was enhanced. The increase of concentration led also to a large increase in viscosity (Fig. 2). Due to the increasing viscosities the mobility of the polymer chains in solutions decreased, the build-up of junction zones decelerated and therefore the slope of the gelation process also decreased.

The data in Figure 4 shows gelation performance of a MC solution at $c = 2\%$ as a function of temperature for different angular frequencies ω. In the low temperature region a strong frequency dependence of G' and G'' was observed. At low temperatures and high frequencies the storage modulus was close to the loss modulus and for the lower frequencies the difference between G' and G'' was getting more distinctive. The data are in good agreement with those given in Fig. 1.

Above 50 °C all storage moduli sharply increase, exceed the loss moduli and converge with each other. This is in good alignment to the work of Winter, who proposed the independence of the gelation process from the applied frequency (Winter & Chambon, 1986). The gelation characteristics were further analyzed according to the methods described for the concentration dependence. These data given in Table 2 indicates an angular frequency dependence of the onset gelation temperature, whereas the cross-over of G' and G'' as well as the slope of inflection of G' are close to frequency independent.

At low frequencies the changes in the deformation take place in such a slow way, that the polymer chains rearrange and stay in a relaxed state. With increasing frequency the available relaxation time declines and the polymer chains get more fixed in their network (Clasen & Kulicke, 2001). Due to the reduced rearrangement possibilities at high frequencies, the mobility of the chains decreases and the assembling of junction zones are prevented,

Table 1
Gelation characteristics based on G' and G'' data as a function of the concentration.

Concentration c (%)	G'_{min} (°C)	Onset gelation temp. (°C)	Cross-over $G' = G''$ (°C)	Inflection point of G' (°C)	Slope at inflection point G' (Pa °C^{-1})	Regression coefficient R^2
1	48	60	61	62	18.7	0.994
2	54	59	60	61	16.6	0.993
3	49	54	56	56	8.4	0.993

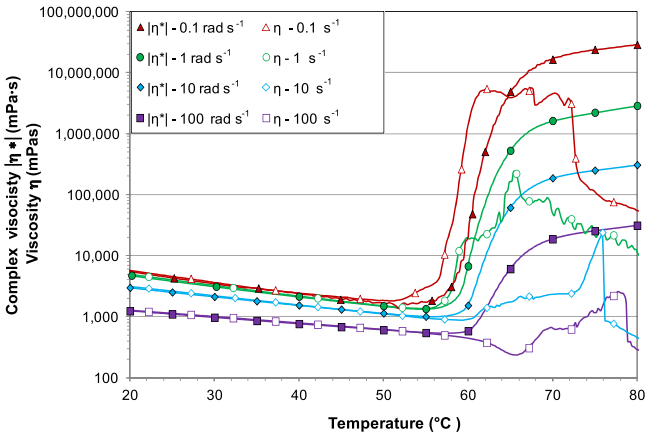

Fig. 5. Steady shear and oscillation flow data according to the shear viscosity η and complex viscosity $|\eta^*|$ as a function of the temperature T of MC at concentrations of 2% for various shear rates $\dot{\gamma}$ and angular frequencies ω in aqueous solutions (heating rate = 1 °C min^{-1}).

leading to increasing onset gelation temperatures. When G' exceeds G'' the polymer chains are fixed inside the gel network and the further parameters show no distinctive frequency dependence.

Besides the common use of oscillation shear flow measurements for methylcellulose gelation analysis (Desbrières et al., 2000; Haque & Morris, 1993; Kobayashi et al., 1999; Li, 2002), some additional authors have also used shear flow measurements to analyze the gelation (Sarkar, 1979; Xu, Song, Ping, Wang, & Liu, 2006).

To this day a clear comparison between the commonly used oscillation flow data vs. shear flow data on the gelation performance of MC is missing. Many industrial processes include a wide variety of the applied shear (Steffe, 1996). Therefore we investigated the gelation process of a MC solution at c = 2% in aqueous solution for a variety of applied shear rates $\dot{\gamma} = 0.1 - 100$ s^{-1} and compared the results of the viscosity η to the complex viscosity $|\eta^*|$ over the corresponding range of the angular frequencies. The results are given in Fig. 5. The gelation temperature characteristics are given in Table 3, evaluated like for the analysis of the concentration dependence of the storage modulus.

In the low temperature region the shear viscosity η and complex viscosity $|\eta^*|$ show a decrease with increasing shear rate rates $\dot{\gamma}$ and the corresponding angular frequencies ω (Fig. 2). Up to a temperature of ~50 °C both material functions show equivalent values and the Cox–Merz rule is fulfilled.

Above 45 °C the gelation causes an increase of the viscosity. As shown from the data of the G' and G'' (Fig. 4 and Table 2) the onset gelation temperatures based on the data of the complex viscosity $|\eta^*|$ increase with the angular frequencies ω. The slope of the gelation curve decreases and the complex viscosities in the high temperature region decrease significantly with ω. Due to the low deformation the oscillation shear flow does not destroy the formation of the MC gel at high temperatures.

For applied shear rates $\dot{\gamma} - 0.1$ s^{-1} and 1 s^{-1} the gelation temperatures were found to be lower than the corresponding to angular frequencies ω = 0.1 rad s^{-1} and 1 rad s^{-1}. Additionally higher slopes at the inflection points were obtained for these shear rates as compared to the angular frequencies. For these shear rates of 0.1 and 1 s^{-1} at low temperatures the viscosity remains in the Newtonian regime, enabling the polymer chains to build up new entanglements at the same time as the others are depleted.

A hypothesis for this decreasing gelation temperature under low shear vs. the corresponding angular frequency could be, the applied shear rate of 0.1–1 s^{-1} leads to an orientation of the polymer coils in solution or the rearrangements of the entanglements between these are leading to a different conformation of the MC in solution. In this new state the hydrophobic groups are able to associate to junction zones at lower temperatures and the gel formation is increased, as seen by the increased slope at the inflection point for $\dot{\gamma} = 0.1 - 1$ s^{-1}.

While the low shear rates shift the formation of junction zones to lower temperatures, shear rates of 10 s^{-1} and 100 s^{-1} cause the gel formation to higher temperatures as for the corresponding angular frequencies ω. The shear rate of 10 s^{-1} is above the critical shear rate which is defined as the onset of the pseudoplastic flow behavior (see Figs. 2 and 5). Here entanglements are depleted as re-build and polymer coils in solutions are further deformed. This has a destructive effect on the formation of the junction zones and the onset gelation temperatures are shifted to higher temperatures as for the corresponding angular frequencies.

With further increasing temperatures all applied shear rate leads to destruction and breakdown of the gel network indicated by the scattering and the additional decline of these viscosity η values.

Many industrial applications include an applied shear force. Therefore the knowledge of the impact of the shear rate on the gelation temperature is critical in order to design and to optimize process parameters.

3.2. The shear dependence of the thermal gelation in ceramic paste

The shear dependence of the thermal gelation in ceramic paste was investigated in an aqueous paste kneading and extrusion process. Gelation of methylcellulose in an aqueous ceramic paste, was first described by Schuetz (1986) measuring the torque increase when the paste was heated up in a torque rheometer. In an extrusion trial, the gelation was observed close to a temperature when defect formation occurred in the extrudate (Bayer & Knarr, 2012; Bayer & Lang, 2012a,b). During the gelation of the methylcellulose, the plasticity of the ceramic paste decreased significantly leading to a sharp increase of the extrusion pressure. The gelation temperature in the paste decreased with the MC concentration and higher MC concentrations often led to a gelation temperature close to or slightly above room temperature (Bayer & Lang, 2012a; Schuetz, 1986). The MC gelation is one reason for defect formation and for speed limitation in industrial paste extrusion processes. The influence of the gelation temperature on the applied shear in ceramic paste has not been reported up to date and this is the second part of our study.

The shear dependence was investigated by performing temperature sweep trials in a torque rheometer and in a single screw extruder. In both cases the ceramic paste was heated up at a constant rate during the trial and different parameters were

Table 2
Gelation characteristics based on G' and G'' data as a function of the angular frequency for MC at c = 2%.

Angular frequency ω (rad s^{-1})	G'_{min} (°C)	Onset gelation temp. (°C)	Cross-over $G' = G''$ (°C)	Inflection point of G' (°C)	Slope at inflection point G' (Pa °C^{-1})	Regression coefficient R^2
0.1	47	57	59	60	15.4	0.958
1	52	58	59	60	17.1	0.992
10	54	59	60	61	16.6	0.993
100	56	60	60	62	13.3	0.993

Table 3
Gelation characteristics based on $|\eta^*|$ and η data as a function of the angular frequency ω and shear rate $\dot{\gamma}$ for MC at $c = 2\%$.

Oscillation mode						Shear rate mode					
Angular freq. ω (rad s^{-1})	$\lvert\eta^*\rvert_{min}$ (°C)	Onset gel temp. $\lvert\eta^*\rvert$ (°C)	Inflec. point $\lvert\eta^*\rvert$ (°C)	Slope at inflec. point $\lvert\eta^*\rvert$ (mPa s °C^{-1})	R^2	Shear rate $\dot{\gamma}$ (s^{-1})	η_{min} (°C)	Onset gel temp. η (°C)	Inflec. point η (°C)	Slope at inflec. point η (mPa s °C^{-1})	R^2
0.1	52	59	60	19.9	0.940	0.1	51	57	59	25.3	0.992
1	54	59	60	17.8	0.992	1	54	58	58	28.8	0.965
10	56	60	61	16.7	0.994	10	59	60	61	8.8	0.998
100	57	61	63	13.9	0.992	100	66	66	67	11.1	0.983

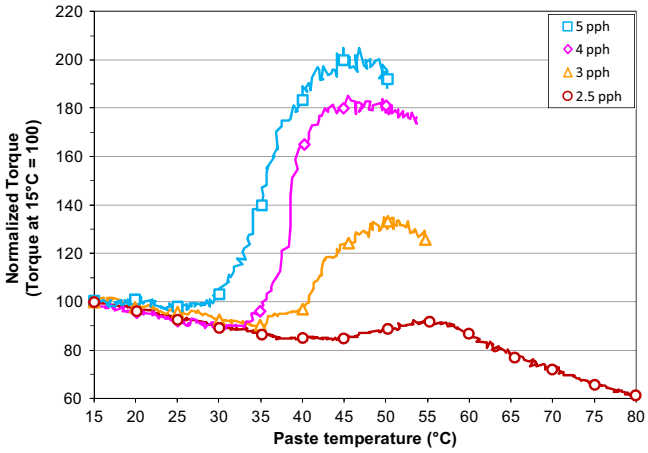

Fig. 6. Temperature sweep trials of a ceramic paste formulation containing different amounts of MC as plasticization aid at a constant kneading speed of 33 rpm (formulation: 100 parts cordierite precursor material, different amounts of MC and 30 parts of water).

determined as a function of the paste temperature. The typical shear rate range of a torque rheometer is normally significantly larger than that of an extruder (in regards of screw speed: two orders of magnitude for the torque rheometer and one for the extruder). However, torque rheometer trials do not allow the direct observation of parameters of the extrusion process like extrusion pressure, speed and the formation of defects in the extrudate. Therefore trials on both devices were performed. In all results presented below, the gelation temperature is defined as the temperature with the lowest torque or extrusion pressure, before these parameters increase or change significantly in slope due to the onset of gelation of the MC in the paste.

In the ideal case, the gelation temperature is measured in the thermal equilibrium at infinitely slow heating rate. Continuous water evaporation from the aqueous pastes, however, requires a reasonably high heating rate. While the water evaporation is negligible during the torque rheometer trials, it can reach larger values during the extrusion tests. Due to a heat transfer delay from the steel equipment (rheometer or extruder cooling/heating jacket and auger) the programmed heating rate (3 °C min^{-1} for the thermostat in the kneading and extrusion trials) does not always lead to the same real paste heating rates. Different lubrication between trials results in different friction. In the kneading trials the real paste heating rates close to the gelation temperature varied between 2.7 and 3.7 °C min^{-1}; in the extrusion trials between 25 and 40 °C they varied between 1.7 and 1.9 °C min^{-1}.

Trials with the torque rheometer were performed by mixing the paste ingredients homogeneously at a temperature between 4 and 5 °C to guarantee the best possible dissolution for the methylcellulose and minimize formation of microgels and associates. After homogenization the paste was first kneaded until a constant torque was reached and then aged for 5 min to ensure no thixotropy would affect the results. Then the paste was heated up with constant heating and rotating speed. The torque was recorded as a function of the kneading time and later recalculated as a function of the kneading temperature. Small temperature fluctuations in the kneading cell during the heating process are the reason for curves progressing partially backwards in the shown relation "torque as a function of the paste temperature" (Figs. 6 and 7). For ease of comparision, the kneading torque was normalized to 100 at a temperature of 15 °C. The real torques at 15 °C as well as the gelation temperatures for other rotating speeds are given in Table 4.

Fig. 6 shows the dependence of the gelation temperature as a function of the MC concentration at a constant shear rate

Table 4
Gelation characteristics of MC in a kneaded ceramic cordierite precursor paste measured at different counter rotating blades speeds of the torque rheometer as an indication of different shear rates and different concentrations. Paste homogenization temperature: 4–5 °C.

MC concentration (pph)[a]	Corresponding MC concentration in the paste[b]/in the water phase[c] (%)	Rotating speed of torque rheometer (rpm)	Torque at 15 °C (Nm)	Paste gelation temperature (°C)
2.5	1.89/7.69	1	3.4	35
2.5	1.89/7.69	3	3.9	36
2.5	1.89/7.69	10	4.6	41
2.5	1.89/7.69	33	5.1	37
2.5	1.89/7.69	100	5.7	45
3	2.26/9.09	1	2.3	29
3	2.26/9.09	3	3.0	33
3	2.26/9.09	10	3.0	33
3	2.26/9.09	33	4.1	36
3	2.26/9.09	100	5.0	39
4	2.99/11.8	1	2.5	25
4	2.99/11.8	3	3.0	28
4	2.99/11.8	10	3.1	29
4	2.99/11.8	33	3.7	33
4	2.99/11.8	100	4.0	37
5	3.70/14.3	1	3.1	25
5	3.70/14.3	3	2.9	26
5	3.70/14.3	10	3.7	28
5	3.70/14.3	33	3.8	29
5	3.70/14.3	100	5.0	35

[a] Calculation of pph: parts of MC per 100 parts of cordierite.
[b] Calculation: (parts MC)/(parts cordierite precursor material + water + MC), all parts are parts per weight.
[c] Calculation: (parts MC)/(parts water + MC).

corresponding to 33 rpm. At the gelation temperature, the torque starts to rise or changes its slope significantly. The gelation temperature decreases with increasing MC concentration, from 37 to 29 °C.

If the MC concentration is kept constant and the applied shear of the system is increased by a higher rotation speed of the counter-rotating blades, the gelation temperature increases (Fig. 7). From 1 rpm to 100 rpm the gelation temperature raises from 29 °C to 39 °C. Concurrently at temperatures above the gelation, the torque rises to a maximum which is greatest at the lowest rotating speed. We assume the three dimensional methylcellulose chain network which is built up above the gelation temperature makes the paste more brittle and decreases the typical lubrication effect of MC. This leads to higher torques. The MC network is affected more at higher rather than at lower shear leading to a lower torque development for higher rotating speeds. The lower the rotation speed, the higher the maximum of the torque curves and the greater the experimental scatter. At lower shear the pastes could build up a larger MC network which is disrupted less frequently than at higher shear.

There is also a progression of the absolute torque data to higher values with increasing shear. This trend is also visible for other MC concentrations. Table 4 summarizes all measured data including the gelation temperatures and results from series not presented in Figs. 6 and 7.

The extrusion trials were performed at different extruder screw speeds (ranging from 4 – 34 rpm) and with different MC concentrations. During all the trials the material was discharged onto a conveyor belt and circulated into the feeder screw until the continuously heated paste reached a temperature of 80 °C in the extruded profile or the extruded cordierite paste lost its plasticity, got too brittle to be extruded or gave large defects. The test method is described in detail in previous works (Bayer & Knarr, 2012). A series of trials with a concentration of 2 pph (corresponding to 1.51% in the paste) are shown in Fig. 8. The results show the increase of the gelation temperature with screw speed.The gelation temperature in the paste increases from 29 °C for 4 rpm to 38 °C for 34 rpm. Further, the highest accessible temperature of extrusion without defect formation in the extrusion profile also increases with auger

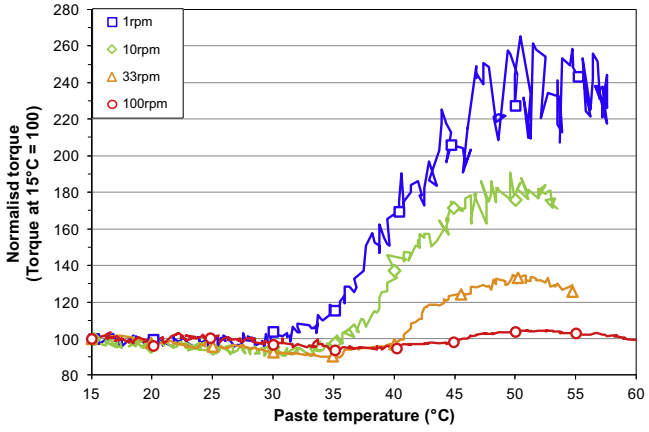

Fig. 7. Temperature sweep trials of a ceramic paste formulation containing 3 pph methylcellulose as plasticization aid at different auger rotating speeds (formulation: 100 parts cordierite, 3 parts MC, 30 parts water).

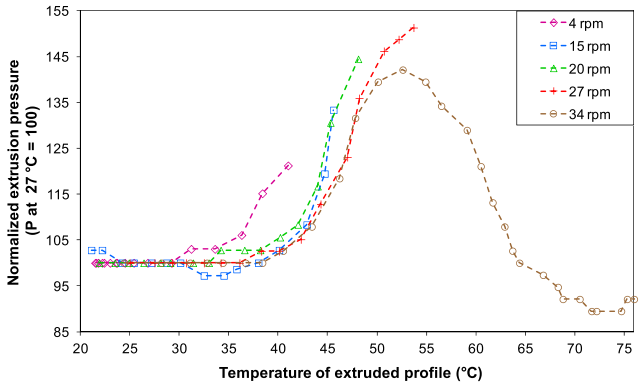

Fig. 8. Temperature sweep trials of a ceramic paste formulation containing MC as plasticization aid at different auger speeds (formulation: 100 parts cordierite precursor material, 2 parts MC and 30.5 parts water); the results of gelation temperatures are listed in Table 5. The extrusion pressures were normalized to 100 at a temperature of 27 °C.

Table 5
Summary of gelation measurements of MC in an extruded ceramic cordierite precursor paste measured at different concentrations, and at different auger screw speeds as an indication of different shear rates. Paste homogenization temperature: 4–5 °C.

MC concentration (pph)[a]	Corresponding MC concentration in the paste[b]/in the water phase[c] (%)	Paste gelation temperature at				
		4 rpm	15 rpm	20 rpm	27 rpm	34 rpm
1	0.076/3.13					≥63[d]
1.5	1.13/4.62		38	46		54
2	1.51/6.15	29	34	33	36	38
4	2.99/11.87	20				27

The data for 20 rpm were taken from Fig. 6.
[a] Calculation of pph: parts of MC per 100 parts of cordierite.
[b] Calculation: (parts MC)/(parts cordierite precursor material + water + MC).
[c] Calculation: (parts MC)/(parts water + MC).
[d] No gelation could be observed until extrusion showed significant defects.
Formulations in parts per weight: 100 parts cordierite + 1 – 4 parts MC + water (31 parts for 1 and 1.5 pph, 30.5 parts for 2 pph, 29.7 parts for 4 pph, 30 parts for 5 pph). Different amounts of water were required to adjust all pastes to comparable paste consistencies, measured with a Shore-A hardness tester to be between 11.3 and 11.6.

speed. The curve at 34 rpm shows a pressure maximum at 53 °C. Similar maxima have been reported earlier and were attributed to formation of intermolecular and/or intramolecular hydrophobic interactions between methyl groups of the polymer chains (Bayer & Knarr, 2012). However, curve (Fig. 8) for a MC with a commercial substitution degree showing a maximum and extrudability up to 80 °C in a ceramic paste has not been reported previously and is contradictory to daily experience in extrusion plant operation. Normally, the gelation of the MC leads to pastes getting so brittle that no further processing at higher temperature is possible. As proposed for the results from the kneading trials, we assume that the high extruder auger speed destroys the three-dimensional hydrophobic network interactions which (under "normal" low shear conditions) make the paste too brittle to be extruded.

For the comparison of gelation temperatures from different temperature sweep trials, it was ensured that all trials were performed under a similar paste heating rate. Due to a large heat transfer delay from the steel made extruder cooling/heating jacket and auger screw, the programmed heating rate (3 °C min^{-1} for the thermostat) did not reflect the real paste heating rate, which was 1.2 °C min^{-1} for all trials in the range of gelation temperatures. Some trials were performed also at different MC concentrations and heating rates. A summary of the gelation temperatures of all trials is given in Table 5. Also at other MC concentrations the gelation temperature increases with the extruder auger screw speed.

4. Conclusions

In this paper, we demonstrate the dependence of the gelation temperature of methylcellulose in aqueous solutions as well as in aqueous ceramic paste on the applied shear. Rheological investigations in oscillation vs. shear mode show lower gelation temperature at low shear rates as for the corresponding angular frequencies. Above the critical shear rate gelation is shifted to higher temperatures. The increase of the gelation temperature of MC with increasing shear could also be validated in the ceramic paste extrusion where MC is used as plastiziser. The problem of defect formation in the extrudates when running close to the gelation temperature can be reduced if the extrusion process is performed under a higher shear rate.

References

Akthar, F. K., & Evans, J. R. G. (2010). High porosity (>90%) cementitious foams. *Cement and Concrete Research*, *40*(2), 352–358.

Bain, M. K., Bhowmick, B., Maity, D., Mondal, D., Mollick, M. M. R., Rana, D., et al. (2012). Synergistic effect of salt mixture on the gelation temperature and morphology of methylcellulose hydrogel. *International Journal of Biological Macromolecules*, *51*(5), 831–836.

Bayer, R., & Knarr, M. (2012). Thermal precipitation or gelling behaviour of dissolved methylcellulose (MC) derivatives—Behaviour in water and influence on the extrusion of ceramic pastes. Part 1: Fundamentals of MC-derivatives. *Journal of the European Ceramic Society*, *32*(5), 1007–1018.

Bayer, R., & Lang, M. (2012a). High-strength and corrosion-resistant alumina tubes through extrusion, part 1. *CFI Ceramic Forum International*, *89*(5). E115-E116, E118-E121.

Bayer, R., & Lang, M. (2012b). High-strength and corrosion-resistant alumina tubes through extrusion, part 2. *CFI Ceramic Forum International*, *89*(6-7), E37–E40.

Bhui, D. K., & Misra, A. (2012). Synthesis of worm like silver nanoparticles in methyl cellulose polymeric matrix and its catalytic activity. *Carbohydrate Polymers*, *89*(3), 830–835.

Bhui, D. K., Pyne, S., Sarkar, P., Bar, H., Sahoo, G. P., & Misra, A. (2011). Temperature controlled synthesis of silver nanostructures of variable morphologies in aqueous methyl cellulose matrix. *Journal of Molecular Liquids*, *158*(3), 170–174.

Castelain, C., Doublier, J. L., & Lefebvre, J. (1987). A study of the viscosity of cellulose derivatives in aqueous solutions. *Carbohydrate Polymers*, *7*(1), 1–16.

Church, B. C., Sanders, T. H., Speyer, R. F., & Cochran, J. K. (2007). Thermal expansion matching and oxidation resistance of Fe–Ni–Cr interconnect alloys. *Materials Science and Engineering: A*, *452–453*(0), 334–340.

Clasen, C., & Kulicke, W. M. (2001). Determination of viscoelastic and rheo-optical material functions of water-soluble cellulose derivatives. *Progress in Polymer Science*, *26*(9), 1839–1919.

Cox, W. P., & Merz, E. H. (1958). Correlation of dynamic and steady flow viscosities. *Journal of Polymer Science*, *28*(118), 619–622.

Denham, W. S., & Woodhouse, H. (1913). CLXXXVI.-The methylation of cellulose. *Journal of the Chemical Society, Transactions*, *103*(0), 1735–1742.

Desbrieres, J., Hirrien, M., & Rinaudo, M. (1998). A calorimetric study of methylcellulose gelation. *Carbohydrate Polymers*, *37*(2), 145–152.

Desbrières, J., Hirrien, M., & Ross-Murphy, S. B. (2000). Thermogelation of methylcellulose: Rheological considerations. *Polymer*, *41*(7), 2451–2461.

Dreyfus, H. (1912). Procédé pour la fabrication d'éthers cellulosiques et de leurs produits de transformation FR Patent 462,274.

Fairclough, J. P. A., Yu, H., Kelly, O., Ryan, A. J., Sammler, R. L., & Radler, M. (2012). Interplay between gelation and phase separation in aqueous solutions of methylcellulose and hydroxypropylmethylcellulose. *Langmuir*, *28*(28), 10551–10557.

Floury, J., Desrumaux, A., Axelos, M. A. V., & Legrand, J. (2003). Effect of high pressure homogenisation on methylcellulose as food emulsifier. *Journal of Food Engineering*, *58*(3), 227–238.

Ford, J. L. (1999). Thermal analysis of hydroxypropylmethylcellulose and methylcellulose: Powders, gels and matrix tablets. *International Journal of Pharmaceutics*, *179*(2), 209–228.

Ford, J. L., & Mitchell, K. (1995). Thermal analysis of gels and matrix tablets containing cellulose ethers. *Thermochimica Acta*, *248*(0), 329–345.

Funami, T., Kataoka, Y., Hiroe, M., Asai, I., Takahashi, R., & Nisbinari, K. (2007). Thermal aggregation of methylcellulose with different molecular weights. *Food Hydrocolloids*, *21*(1), 46–58.

Glasser, W., Atalla, R., Blackwell, J., Malcolm Brown, R., Jr., Burchard, W., French, A., et al. (2012). About the structure of cellulose: Debating the Lindman hypothesis. *Cellulose*, *19*(3), 589–598.

Haque, A., & Morris, E. R. (1993). Thermogelation of methylcellulose. Part I: Molecular structures and processes. *Carbohydrate Polymers*, *22*(3), 161–173.

Heymann, E. (1935). Studies on sol-gel transformations. I. The inverse sol–gel transformation of methylcellulose in water. *Transactions of the Faraday Society*, *31*, 846–864.

Hirrien, M., Chevillard, C., Desbrières, J., Axelos, M. A. V., & Rinaudo, M. (1998). Thermogelation of methylcelluloses: New evidence for understanding the gelation mechanism. *Polymer*, *39*(25), 6251–6259.

Hofmeister, F. (1888). Zur Lehre von der Wirkung der Salze. *Archiv für experimentelle Pathologie und Pharmakologie*, *24*(4–5), 247–260.

Iso, N., & Yamamoto, D. (1970). Effects of sucrose and citric acid on the sol–gel transformation of methylcellulose in water. *Agricultural and Biological Chemistry*, *34*, 1867–1869.
Kandasamy, P., Varadharaju, N., Kalemullah, S., & Maladhi, D. (2012). Optimization of process parameters for foam-mat drying of papaya pulp. *Journal of Food Science and Technology*, 1–9.
Kato, T., Yokoyama, M., & Takahashi, A. (1978). Melting temperatures of thermally reversible gels. 4. Methyl cellulose-water gels. *Colloid and Polymer Science*, *256*(1), 15–21.
Knarr, M., Adden, R., Anderson, W. H. K., & Hübner-Keese, B. (2012). Characterization of in-vitro gel performance of novel MC with respect to the suitability for satiety applications. *Food Hydrocolloids*, *29*(2), 317–325.
Kobayashi, K., Huang, C. I., & Lodge, T. P. (1999). Thermoreversible gelation of aqueous methylcellulose solutions. *Macromolecules*, *32*(21), 7070–7077.
Kulicke, W. M., & Porter, R. S. (1980). Relation between steady shear flow and dynamic rheology. *Rheologica Acta*, *19*(5), 601–605.
Kundu, P. P., & Kundu, M. (2001). Effect of salts and surfactant and their doses on the gelation of extremely dilute solutions of methyl cellulose. *Polymer*, *42*(5), 2015–2020.
Levy, G., & Schwarz, T. W. (1958). The effect of certain additives on the gel point of methylcellulose. *Journal of the American Pharmaceutical Association*, *47*(1), 44–46.
Li, L. (2002). Thermal gelation of methylcellulose in water: Scaling and thermoreversibility. *Macromolecules*, *35*(15), 5990–5998.
Li, L., Thangamathesvaran, P. M., Yue, C. Y., Tam, K. C., Hu, X., & Lam, Y. C. (2001). Gel network structure of methylcellulose in water. *Langmuir*, *17*(26), 8062–8068.
Li, L., Shan, H., Yue, C. Y., Lam, Y. C., Tam, K. C., & Hu, X. (2002). Thermally induced association and dissociation of methylcellulose in aqueous solutions. *Langmuir*, *18*(20), 7291–7298.
Lilienfeld, L. (1912a). Alkyl ethers of cellulose and process of making the same. US Patent 1,188,376.
Lilienfeld, L. (1912b). A process for the manufacture and production of ethers of cellulose, its conversion products and derivatives. GB Patent 1912, 12,854.
Lilienfeld, L. (1912c). Verfahren zur Darstellung von Äthern der Cellulose. D.R.P. (DE) Patent 477,154.
Liu, S. Q., Joshi, S. C., Lam, Y. C., & Tam, K. C. (2008). Thermoreversible gelation of hydroxypropylmethylcellulose in simulated body fluids. *Carbohydrate Polymers*, *72*(1), 133–143.
Medronho, B., Romano, A., Miguel, M., Stigsson, L., & Lindman, B. (2012). Rationalizing cellulose (in)solubility: Reviewing basic physicochemical aspects and role of hydrophobic interactions. *Cellulose*, *19*(3), 581–587.
Morris, E. R., Cutler, A. N., Ross-Murphy, S. B., Rees, D. A., & Price, J. (1981). Concentration and shear rate dependence of viscosity in random coil polysaccharide solutions. *Carbohydrate Polymers*, *1*(1), 5–21.
Nishida, R., & Takahashi, M. (2008). Self-assembled orientation of polymer chains in methylcellulose gel during drying process. *Polymer Journal*, *40*(2), 148–153.
Ou, Z. H., Ma, B. G., & Jian, S. W. (2012). Influence of cellulose ethers molecular parameters on hydration kinetics of Portland cement at early ages. *Construction and Building Materials*, *33*, 78–83.
Pusz, J., Smirnova, A., Mohammadi, A., & Sammes, N. M. (2007). Fracture strength of micro-tubular solid oxide fuel cell anode in redox cycling experiments. *Journal of Power Sources*, *163*(2), 900–906.
Robinson, G., Ross-Murphy, S. B., & Morris, E. R. (1982). Viscosity–molecular weight relationships, intrinsic chain flexibility, and dynamic solution properties of guar galactomannan. *Carbohydrate Research*, *107*(1), 17–32.
Rogers, T. L., & Wallick, D. (2012). Reviewing the use of ethylcellulose, methylcellulose and hypromellose in microencapsulation. Part 1: Materials used to formulate microcapsules. *Drug Development and Industrial Pharmacy*, *38*(2), 129–157.
Ross-Murphy, S. B. (1995). Structure–property relationships in food biopolymer gels and solutions. *Journal of Rheology*, *39*(6), 1451–1463.
Sarkar, N. (1979). Thermal gelation properties of methyl and hydroxypropyl methylcellulose. *Journal of Applied Polymer Science*, *24*(4), 1073–1087.
Sarkar, N. (1995). Kinetics of thermal gelation of methylcellulose and hydroxypropylmethylcellulose in aqueous solutions. *Carbohydrate Polymers*, *26*(3), 195–203.
Schuetz, J. E. (1986). Methylcellulose polymers as binders for extrusion of ceramics. *American Ceramic Society Bulletin*, *65*(12), 1556–1559.
Staudinger, H., & Schweitzer, O. (1930). Über hochpolymere Verbindungen, 40. Mitteil.: Viscositäts-Messungen an Polysacchariden und Polysaccharid-Derivaten. *Berichte der deutschen chemischen Gesellschaft (A and B Series)*, *63*(8), 2317–2330.
Steffe, J. F. (1996). *Rheological methods in food process engineering*. East Lansing, MI, USA: Freeman Press.
Takahashi, M., Shimazaki, M., & Yamamoto, J. (2001). Thermoreversible gelation and phase separation in aqueous methyl cellulose solutions. *Journal of Polymer Science Part B: Polymer Physics*, *39*(1), 91–100.
Takeshita, H., Saito, K., Miya, M., Takenaka, K., & Shiomi, T. (2010). Laser speckle analysis on correlation between gelation and phase separation in aqueous methyl cellulose solutions. *Journal of Polymer Science Part B: Polymer Physics*, *48*(2), 168–174.
Wang, Q., & Li, L. (2005). Effects of molecular weight on thermoreversible gelation and gel elasticity of methylcellulose in aqueous solution. *Carbohydrate Polymers*, *62*(3), 232–238.
Wang, Q., Li, L., Chen, G., & Yang, Y. (2007). Effects of magnetic field on the sol–gel transition of methylcellulose in water. *Carbohydrate Polymers*, *70*(3), 345–349.
Winter, H. H., & Chambon, F. (1986). Analysis of linear viscoelasticity of a crosslinking polymer at the gel point. *Journal of Rheology*, *30*(2), 367–382.
Xu, Y., Li, L., Zheng, P., Lam, Y. C., & Hu, X. (2004). Controllable gelation of methylcellulose by a salt mixture. *Langmuir*, *20*(15), 6134–6138.
Xu, X. M., Song, Y. M., Ping, Q. N., Wang, Y., & Liu, X. Y. (2006). Effect of ionic strength on the temperature-dependent behavior of hydroxypropyl methylcellulose solution and matrix tablet. *Journal of Applied Polymer Science*, *102*(4), 4066–4074.